Pressure-area isotherm of a lipid monolayer from molecular dynamics simulations

Baoukina, Svetlana; Monticelli, Luca; Marrink, Siewert J.; Tieleman, D. Peter

[Link to publication in University of Groningen/UMCG research database](#)

Pressure−Area Isotherm of a Lipid Monolayer from Molecular Dynamics Simulations

Svetlana Baoukina,[†] Luca Monticelli,[†] Siewert J. Marrink,[‡] and D. Peter Tieleman*,[†]

Department of Biological Sciences, University of Calgary, 2500 University Drive Northwest, Calgary, Alerta, Canada, T2N 1N4 and Groningen Biomolecular Sciences and Biotechnology Institute, Department of Biophysical Chemistry, University of Groningen, Nijenborgh 4, 9747 AG

We calculated the pressure−area isotherm of a dipalmitoyl-phosphatidylcholine (DPPC) lipid monolayer from molecular dynamics simulations using a coarse-grained molecular model. We characterized the monolayer structure, geometry, and phases directly from the simulations and compared the calculated isotherm to experiments. The calculated isotherm shows liquid-expanded and liquid-condensed phases and their coexistence plateau. At high pressure, the monolayer surface is rippled; upon further compression, the monolayer undergoes a collapse. We studied the effect of temperature and system size on the isotherm slope and phase coexistence region. Thermodynamic and dynamic properties of the monolayer phases were also investigated.

Introduction

Lipid monolayers are surfactant films formed at hydrophobic−hydrophilic interfaces. They play important roles in a range of heterogeneous systems and are of biological interest for understanding the function of lung surfactant. Monolayers are characterized experimentally by their pressure−area isotherm.[1] Dipalmitoyl-phosphatidylcholine (DPPC) is one of the most studied lipids, and its properties are well understood. At a given temperature, a DPPC monolayer adopts several distinct phases as the area per lipid molecule decreases and the lateral pressure increases: the gas, liquid-expanded (LE), and liquid-condensed (LC) phases. However, the experimentally measured pressure−area isotherms for DPPC monolayers may differ. For example, in the high-pressure region, the isotherm may depend on the experimental method (e.g., Langmuir trough or captive bubble surfactometer) and the experimental details (e.g., monolayer compression rate). The discrepancy arises[2] from differences in monolayer structure and morphology (e.g., the presence of metastable domains or rippled surface of the monolayer) and also because of the loss of material from the interface (e.g., partial monolayer collapse or monolayer leakage), factors which are difficult to control in experiments.

A direct investigation of the structure and dynamics of lipids as a function of monolayer area is not possible via experiments but can be obtained from simulations. Previous simulations of lipid monolayers, using both atomistic[3−7] and coarse-grained[8,9]

models, investigated a limited number of state points on either detailed, very small systems or large, highly idealized systems. In the present work, we calculate the entire pressure−area isotherm of a realistic DPPC lipid monolayer from molecular dynamics (MD) simulations. This study provides information on the monolayer structure and topology, which can be directly compared to experimental studies via the pressure−area isotherms. The coarse-grained model[10] we used in this study accurately reproduces structural and dynamic properties of lipids as well as lipid phase transitions.[11−13]

Methods

General System Setup. The simulation setup included a water slab bounded by two vacuum slabs with two symmetric monolayers at the two vacuum−water interfaces. First, a set of initial structures with different areas per lipid molecule, A_L, in the monolayer was obtained. To this end, a starting structure was compressed or expanded in the lateral direction to change the area of the vacuum−water interfaces without changing the box size in the normal direction. Then, using the initial structures, the properties of the monolayers with different areas per lipid were investigated. To this end, simulations at constant volume of the simulation box were performed with constant areas of the two interfaces and a fixed box size in the direction normal to the interfaces. We simulated a small system containing 64 DPPC/monolayer and a large system containing 4096 DPPC/monolayer. The small system was simulated at 285, 300, and 310 K, the large system was simulated at 300 K.

The surface tension in the monolayer, γ_m, was calculated from the average surface tension in the system given by the difference of the normal, P_N, and lateral, P_L, pressures in the box: $\gamma_m = (P_N - P_L) \cdot L_z / 2$, where L_z is the box normal size and $P_L = (P_{xx} + P_{yy})/2$. The calculated surface tension in the monolayer, γ_m, at a given area per lipid, A_L, provides a point on the tension−area isotherm $\gamma_m(A_L)$. The corresponding pressure−area isotherm is given by the standard relation: $\Pi(A_L) = \gamma_{aw} - \gamma_m(A_L)$, where γ_{aw} denotes the surface tension of the vacuum−water interface.

* To whom correspondence should be addressed. E-mail: tieleman@ucalgary.ca.

† University of Calgary.

‡ University of Groningen.

(1) Kaganer, V. M.; Mohwald, H.; Dutta, P. *Rev. Modern Phys.* **1999**, *71*, 779−819.

(2) Wustneck, R.; Perez-Gil, J.; Wustneck, N.; Cruz, A.; Fainerman, V. B.; Pison, U. *Adv. Colloid Interface Sci.* **2005**, *117*, 33−58.

(3) Dominguez, H.; Smondyrev, A. M.; Berkowitz, M. L. *J. Phys. Chem. B* **1999**, *103*, 9582−9588.

(4) Kaznessis, Y. N.; Kim, S. T.; Larson, R. G. *Biophys. J.* **2002**, *82*, 1731−1742.

(5) Knecht, V.; Muller, M.; Bonn, M.; Marrink, S. J.; Mark, A. E. *J. Chem. Phys.* **2005**, *122*, 024704.

(6) Mauk, A. W.; Chaikof, E. L.; Ludovice, P. J. *Langmuir* **1998**, *14*, 5255−5266.

(7) Siepmann, J. I.; Karaborni, S.; Klein, M. L. *J. Phys. Chem.* **1994**, *98*, 6675−6678.

(8) Adhangale, P. S.; Gaver, D. P. *Mol. Phys.* **2006**, *104*, 3011−3019.

(9) Nielsen, S. O.; Lopez, C. F.; Moore, P. B.; Shelley, J. C.; Klein, M. L. *J. Phys. Chem. B* **2003**, *107*, 13911−13917.

(10) Marrink, S. J.; Risselada. J.; Yefimov, S.; Tieleman, D. P.; de Vries, A. H. *J. Phys. Chem. B* **2007**, *111*, 7812−7824.

(11) Marrink, S. J.; Mark, A. E. *J. Am. Chem. Soc.* **2003**, *125*, 11144−11145.

(12) Marrink, S. J.; Mark, A. E. *Biophys. J.* **2004**, *87*, 3894−3900.

(13) Marrink, S. J.; Risselada, J.; Mark, A. E. *Chem. Phys. Lipids* **2005**, *135*, 223−244.

To compare the calculated isotherm to experimental isotherms, $\Pi^{EXP}(A_L)$, we used an effective surface tension $\gamma_{aw}*$ as an adjustable parameter, so that the relation $\Pi^{EXP}(A_L) = \gamma_{aw}* - \gamma_m(A_L)$ holds approximately for the entire isotherm. The effective surface tension compensates for the difference between the experimental value of the surface tension at the air–water interface and the value of the surface tension of the vacuum–water interface in the CG model. The value of this adjustable parameter can vary depending on the temperature and size of the simulation system.

The calculated isotherms were compared to experimental isotherms measured for DPPC on a captive bubble surfactometer.[14] In this experimental setting, lipid monolayer was formed on the surface of an air bubble in water subphase. Interfacial area was varied through the bubble volume by changing hydrostatic pressure in the chamber. Surface tension was calculated based on the bubble geometry. The 0.05–0.08 μL solution of DPPC in chloroform/methanol (2/1) was spread on the surface of the 80 μL bubble in a 2.5 mL subphase. The subphase contained 10 mM HEPES pH 7.0, 1.5 mM $CaCl_2$, and 150 mM NaCl. The temperature was maintained within ± 0.1 °C of the target value. Surface pressure and area were recorded during isothermal compression at a constant rate of <2.5 Å^2/molecule·min. The captive bubble surfactometer is advantageous over the Langmuir trough setting at high pressures because it prevents loss of material via monolayer leakage (or creepage) at pressures above 55 mN/m and provides directly the total monolayer area instead of the projected area of the (rippled) monolayer over the trough. We notice that in both experimental techniques the calculated area may still differ from the true monolayer area at high pressures due to partial collapse of the monolayer and formation of 3D structures.[2]

Simulation Details. We used a prereleased version of the MARTINI force field,[10] a coarse-grained (CG) model for biomolecular simulations. DPPC is a standard component of the force field. For nonbonded interactions, the standard cutoffs for the CG force field were used: the Lennard–Jones interactions were shifted to zero between 0.9 and 1.2 nm, while the Coulomb potential was shifted to zero between 0 and 1.2 nm. The relative dielectric constant was 15.

Molecular dynamics simulations were performed using the GROMACS (v. 3.3.1) simulation package.[15] The small system contained 128 DPPC molecules and 1746 water particles; the large system contained 8192 DPPC molecules and 111 744 water particles. In the starting structure, the area per lipid molecule in the monolayer was 0.715 nm^2. The box size was $6.8 \times 6.8 \times 20$ nm for the small system and $54 \times 54 \times 75$ nm for the large system. The monolayers at different areas per lipid were obtained from the starting structure using the following procedure. For the large system, the starting structure was compressed by applying a lateral pressure of 5 bar for 40 ns. A set of initial structures for the isotherm was obtained using various time frames from the compression run. For the small system, the starting structure was compressed or expanded with a set of different lateral pressures (−60 to +60 bar) for 100 ns. Positive pressures were used to reduce the area of the interfaces and compress the monolayers; negative pressures were used to increase the interfacial area and expand the monolayer. As a result, monolayers with areas per lipid in the range 0.40–0.85 nm^2 for the small system and 0.46 –0.72 nm^2 for the large system were obtained. Then, for each area per lipid, simulations at constant volume and temperature were performed. The small systems were simulated for 1 μs (200 ns equilibration run, 800 ns production run). The large systems were simulated for 400 ns (200 ns initial equilibration, 200 ns production run). The times reported here are formal simulation times. The effective time sampled by the CG model is larger than the simulation time due to the smooth interaction potentials. On the basis of the diffusion dynamics of the CG water and lipids, the time axis should be rescaled by a factor of 4.[16] Hence, a conversion factor of 4 was applied to calculate the dynamic characteristics of lipid motions.

A time step of 40 fs for small systems and 20 fs for large systems was used. The smaller time step of 20 fs was chosen for the systems with large number of particles to improve the stability of the simulations. The neighbor list was updated every 10 steps. DPPC and water were coupled separately to a Berendsen heat bath[17] with a coupling constant of 1 ps. The monolayer compression/expansion was simulated using semi-isotropic pressure coupling (Berendsen coupling scheme, coupling constant of 4 ps, compressibility in the lateral direction of 5×10^{-5} bar^{-1}) with a fixed box size normal to the membrane. This ensures the thickness of the vacuum slabs in the box changes as the area of the monolayer changes without changing the size of the box normal to the membrane.

For calculations of the surface tension at the vacuum–water interface, the simulation setup included a water cube $20 \times 20 \times 20$ nm containing 33 248 water particles in a $20 \times 20 \times 30$ nm simulation box. For calculation of the surface tension at the lipid chain–vacuum interface, the simulation box contained two layers with 128 lipid chains in each layer (each chain containing 4 hydrocarbon particles, i.e., 1024 particles in total) bound by vacuum slabs on both sides. For each chain position restraints were applied to one of the ends. For calculation of the surface tension at the lipid chain–water interface, 1593 waters were added to the lipid chains. All simulations were performed at constant volume and temperature.

Results

To investigate the effect of temperature and system size on the monolayer surface tension as a function of the area per lipid, we simulated a small system (64 DPPC/monolayer) at 285, 300, and 310 K and a large system (4096 DPPC/monolayer) at 300 K.

First, we simulated the small monolayer at 300 K. The calculated surface tension–area isotherm, $\gamma_m(A_L)$, is shown in Figure 1A. Each point of the isotherm is obtained from a 1 μs simulation of the monolayers at constant area. There are four distinct phase regions in the isotherm. For molecular areas in the range $A_L = 0.72$–0.84 nm^2, the monolayer in liquid-expanded (LE) phase coexists with pores. The pores form on the nanosecond time scale and are stable during the simulation time. For areas per lipid in the range $A_L = 0.55$–0.72 nm^2, the monolayer is in the LE phase with no pores. The monolayers with molecular areas in the range $A_L = 0.49$–0.55 nm^2 could not be reproduced by applying any surface tension/lateral pressure (see Methods). This region corresponds to the coexistence of LE and liquid-condensed (LC) monolayer phases. The monolayers cannot phase separate in the simulations because of the small system size. In this region, nucleation of the second phase would not take place and the small monolayer would exist in only one metastable phase with intermediate (between the LC and LE phases) properties. For areas per lipid in the range 0.47–0.49 nm^2, the monolayer is in the LC phase. Note that the monolayer surface tension changes sign in this region and reaches large negative values. The monolayers with negative surface tensions are unstable. In the simulations, the monolayer is trapped on the interface in the flat geometry and does not collapse. The size of the simulated system is too small to develop collective out-of-plane displacements of the lipids (monolayer bending). Displacements of individual lipids (lipid protrusions) occur at more negative tensions and lead to collapse of the monolayer (data not shown).

Second, we simulated the small system at 285 and 310 K. The calculated tension–area isotherms are shown in Figure 1A for a smaller interval of molecular areas. The surface tension in the monolayer decreases with the increase of temperature, while the width of the LC–LE phase coexistence region does not change noticeably.

(14) Crane, J. M.; Putz, G.; Hall, S. B. *Biophys. J.* **1999**, *77*, 3134–3143.
(15) Lindahl, E.; Hess, B.; van der Spoel, D. *J. Mol. Model.* **2001**, *7*, 306–317.
(16) Marrink, S. J.; de Vries, A. H.; Mark, A. E. *J. Phys. Chem. B* **2004**, *108*, 750–760.

(17) Berendsen, H. J. C.; Postma, J. P. M.; van Gunsteren, W. F.; DiNola, A.; Haak, J. R. *J. Chem. Phys.* **1984**, *81*, 3684–3690.
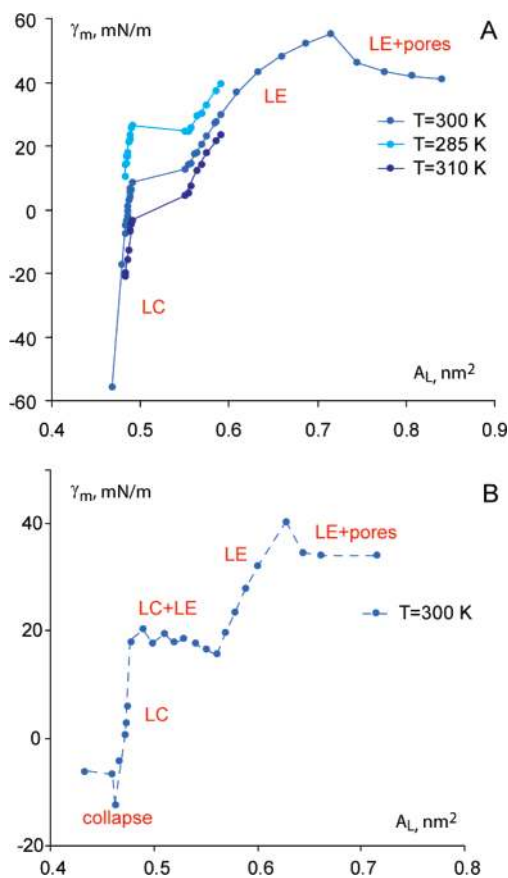
Figure 1. Tension−area isotherms for a DPPC monolayer from molecular dynamics simulations for (A) a small system (64 DPPC/ monolayer) and (B) a large system (4096 DPPC/monolayer). The isotherms show liquid-expanded (LE) phase with pores, LE phase, liquid-condensed (LC) phase, the coexistence of LC and LE phases, and monolayer collapse plateau. Estimate of the error for monolayer tension is <0.3 mN/m.

Next, we simulated the large system at 300 K. The calculated tension−area isotherm $\gamma_m(A_L)$ is shown in Figure 1B. The structure of the monolayer corresponding to different phase regions of the isotherm is shown in Figure 2. For large molecular areas ($A_L = 0.63−0.72$ nm^2) the monolayer forms a LE phase with stable pores. Pore formation is observed at smaller areas per lipid compared to the small system. A similar tendency but at larger areas per lipid (~1.00 nm^2) is also found in the atomistic simulations of DPPC monolayers.[5]

Highly compressed monolayers (at $A_L = 0.43−0.46$ nm^2) have negative surface tension and are unstable on the interface. The monolayer surface becomes rippled already at $A_L = 0.467$ nm^2 (Figure 3A). At this point, the monolayer true area starts to deviate from the area projected on the interface. As a result, the slope of the isotherm becomes less steep. Upon further decrease of the monolayer area, the monolayer out-of-plane deviations grow in amplitude. The monolayer bending deformation is accompanied by partial loss of lipids into water (Figure 3B). This corresponds to a collapse plateau on the isotherm (Figure 1B).

For lipid areas in the interval $A_L = 0.56−0.63$ nm^2, the monolayer forms a LE phase (Figure 2). This phase is characterized by the absence of long-range translational order and orientational disorder of the lipid chains. For areas in the range $A_L = 0.46−0.48$ nm^2, the monolayer forms a LC phase (Figure 2). This phase is characterized by hexagonal packing and increased orientational ordering of the hydrocarbon chains. The order parameter profiles for the bonds between coarse-grained

particles constituting a DPPC molecule (including lipid head group and both hydrocarbon chains) with respect to the monolayer normal are shown in Figure 4A. The order parameter for the hydrocarbon chains is significantly higher in the LC phase than in the LE phase. The radial distribution function for the hydrocarbon chains in the LC phase has an oscillatory form (Figure 4B). The range of the correlations increases strongly in the LC phase compared to the LE phase, indicating substantial long-range translational ordering of the hydrocarbon chains. To investigate the dynamics of translational motions in the two phases, we also calculated the coefficient of (long time) lateral diffusion of DPPC molecules. For the monolayers in the LE phase, the diffusion coefficient increases slightly with the increase of area per lipid: $D = (2.4 \pm 0.1) \times 10^{-7}$ cm^2/s (at $A_L = 0.57$ nm^2) and $D = (3.3 \pm 0.1) \times 10^{-7}$ cm^2/s (at $A_L = 0.63$ nm^2). Both values are similar to the diffusion coefficients of DPPC molecules in bilayers in the liquid-crystalline phase obtained in experiments[18] and in simulations.[16,19] In the LC phase, the diffusion coefficient decreases by 2 orders of magnitude: $D = (1.4 \pm 0.1) \times 10^{-9}$ cm^2/s (at $A_L = 0.475$ nm^2) compared to the LE phase. This drop in the diffusion coefficient is also similar to the experimental measurements and simulation results for DPPC bilayers in the gel phase.[13]

Interestingly, the phase coexistence is also reproduced in the simulations of the large monolayers. The LC phase coexists with the LE phase in monolayers with areas per lipid $A_L = 0.48−0.56$ nm^2 (Figure 1B, plateau region on the isotherm). At each point on the plateau, domains of both phases are observed (Figure 2). To identify the lipids belonging to the LC and LE domains, Voronoi analysis was performed on the hydrocarbon chains. A lipid chain was defined to be in the LC phase if the C2 particle in the chain had six neighbors within a distance of 1 nm. Two lipid chains were determined to belong to the same domain if the distance between them was smaller than 0.53 nm. The results of the Voronoi analysis are shown in Figure 5 for a monolayer at $A_L = 0.51$ nm^2. Initially, small domains of the LC and LE phases are formed, which then diffuse and grow in size, until the separation is complete, resulting in two infinite stripes of the two phases, spanning the simulation box.

From the slopes of the tension−area isotherms, we estimated the area compressibility modulus, K_A, of the monolayers. The following formula was used: $K_A = A_L \cdot \partial \gamma_m / \partial A_L$. In the LC phase, the slope of the isotherm does not change significantly. The values of the area compressibility moduli at $A_L = 0.475$ nm^2 are $K_A = 1800 \pm 20$ and 1400 ± 20 mN/m in the small and large monolayers, respectively. In the LE phase, the area compressibility modulus decreases as the monolayer becomes more expanded. For the small monolayer, the values of the area compressibility modulus vary between $K_A = 250 \pm 30$ (at $A_L = 0.58$ nm^2) and 150 ± 10 (at $A_L = 0.620$ nm^2) and 60 ± 10 (at $A_L = 0.715$ nm^2). For the large monolayer, the values of the area compressibility modulus decrease from $K_A = 200 \pm 12$ (at $A_L = 0.58$ nm^2) to 100 ± 10 mN/m (at $A_L = 0.620$ nm^2). The area compressibility modulus of a monolayer can be compared to that of a bilayer by simply multiplying its value by two. The calculated values for the monolayer area compressability moduli in the LE phase agree well with the experimental[20] and simulation[21,22] data on liquid-crystalline DPPC bilayers.

In order to transform the calculated monolayer tension−area isotherm to a pressure−area isotherm, we first calculated the

(18) Kuo, A. L.; Wade, C. G. *Biochemistry* **1979**, *18*, 2300−2308.
(19) Wohlert, J.; Edholm, O. *J. Chem. Phys.* **2006**, *125*, 204703.
(20) Evans, E.; Rawicz, W. *Phys. Rev. Lett.* **1990**, *64*, 2094−2097.
(21) Lindahl, E.; Edholm, O. *Biophys. J.* **2000**, *79*, 426−433.
(22) Marrink, S. J.; Mark, A. E. *J. Phys. Chem. B* **2001**, *105*, 6122−6127.
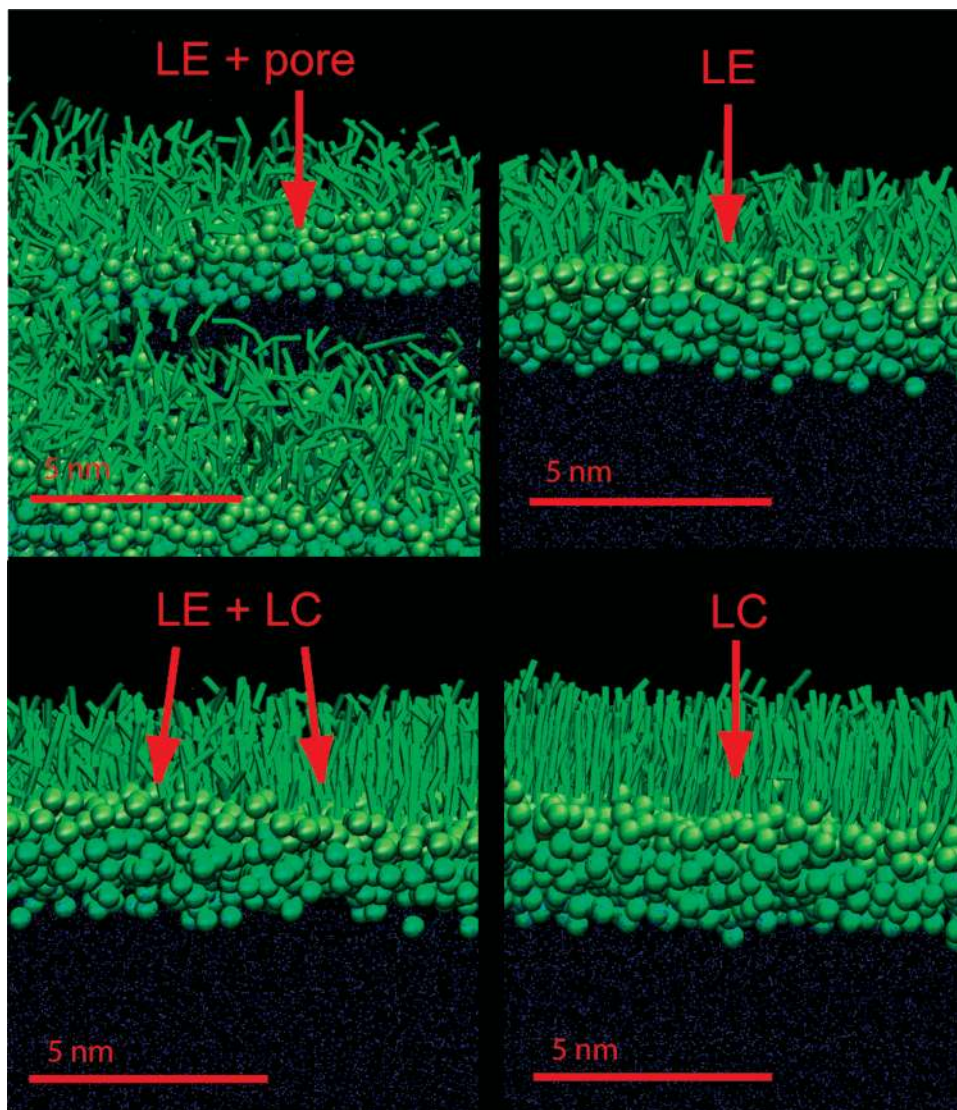
Figure 2. Snapshots from the simulations of DPPC monolayers (the large system, 4096 DPPC/monolayer) in liquid-expanded (LE) and liquid-condensed (LC) phases, their coexistence region (LC + LE) (side view), and LE phase with pores (top view).

surface tensions obtained with the coarse-grained (CG) model at the following interfaces: lipid chain−water, lipid chain−vacuum, and vacuum−water. The calculated surface tensions at lipid chain−water and lipid chain−vacuum interfaces are 43 and 22 mN/m, respectively, in good agreement with experimental values for bulk alkanes[23] (52 and 22 mN/m, respectively). The calculated surface tension at the vacuum−water interface γ_{aw}^{CG} = 32 mN/m, however, is substantially lower than the experimental value of the surface tension at the air−water interface: γ_{aw}^{EXP} = 72 mN/m. Therefore, the relation between the pressure and the tension in the monolayer, $\Pi(A_L) = \gamma_{aw} - \gamma_m(A_L)$, cannot be applied directly for the calculated isotherm. A correction is required to compensate for this difference in surface tensions. Here, we chose this correction in the simple form $\Pi^{EXP}(A_L) = \gamma_{aw}^* - \gamma_m(A_L)$ with an the effective surface tension $\gamma_{aw}^* = $ const. We fit the calculated isotherm to the constant-pressure plateau in the experimental curves corresponding to the LE−LC phase coexistence region. In the experimental curves, the width of the LC−LE coexistence plateau decreases and the transition pressure increases with increasing temperature. In the simulations, the expected decrease of the plateau width with increasing

temperature is not observed. The best fit of the calculated isotherm ($T = 300$ K) for the large system is obtained to the experimental isotherm at $T = 310$ K by setting $\gamma_{aw}^* = 55$ mN/m (Figure 6). These two curves have comparable width of the LC−LE coexistence region as both temperatures are close to their respective main phase transition temperatures, T_m, in the bilayers (295 K in the CG model[13] and 314 K in experiments). For the small system, the best fit is obtained with a smaller value of the effective surface tension $\gamma_{aw}^* = 47$ mN/m.

Discussion

Molecular dynamic simulations can complement experimental data on lipid monolayers by providing atomic-level information on the monolayer properties. In previous simulations of lipid monolayers several important features have already been captured. Monolayer self-assembly[24] and collapse[9] were simulated. The structure and dynamics of monolayers forming the LC, LE, and gas phases were investigated.[4−6,8,9] However, in these works only a limited number of state points for small systems (~100 lipids, box lateral size ≈ 10 nm) have been studied.

(23) Aveyard, R.; Haydon, D. A. *An Introduction to the Principles of Surface Chemistry*; Cambridge University: New York, 1973.

(24) Lopez, C. F.; Nielsen, S. O.; Moore, P. B.; Shelley, J. C.; Klein, M. L. *J. Phys.: Condens. Matter* **2002**, *14*, 9431−9444.
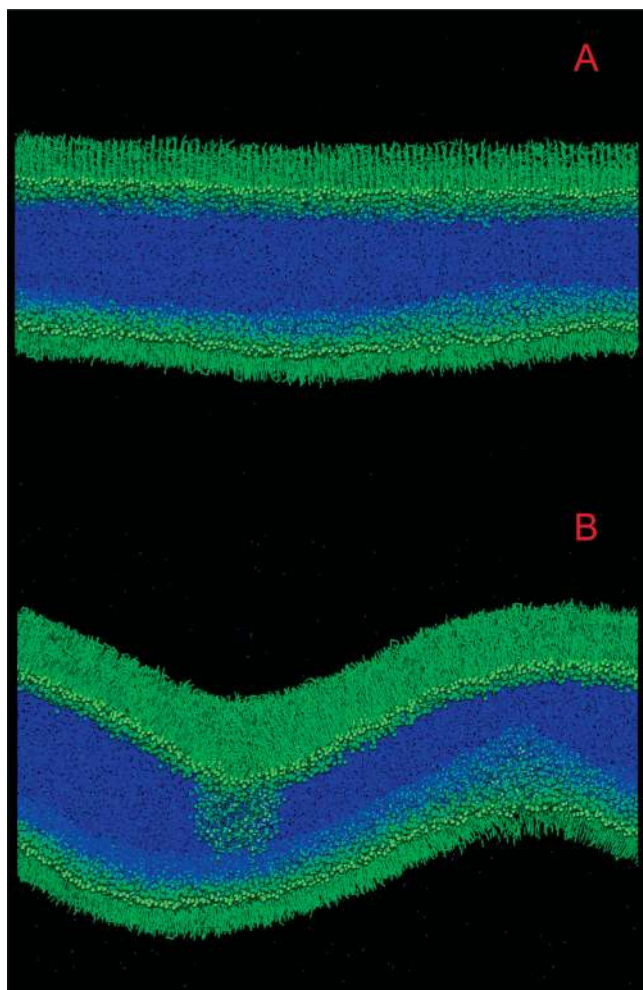
Figure 3. (A) The surface of DPPC monolayers becomes rippled at area per lipid $A_L = 0.467$ nm^2. (B) Upon further compression ($A_L < 0.46$ nm^2), the monolayers undergo bending deformation with partial loss of material from the interface to water.

Figure 4. (A) Orientational order parameter profile for the bonds between coarse-grained particles constituting a DPPC molecule (for lipid head group and both hydrocarbon chains) and (B) radial distribution function for hydrocarbon chain ends (C4 particles) are shown for the monolayers in liquid-expanded (LE) phase, liquid-condensed (LC) phase, and their coexistence region.

In the present work, we systematically studied the phase behavior of the DPPC monolayer. We calculated the entire tension−area isotherm for both small (64 lipids) and large (4096 lipids) systems (Figure 1A,B). The calculated isotherms show distinct phase regions with different thermodynamic and dynamic properties as the area per lipid in the monolayer varies. In the LE phase, lipid chains are disordered; there is no long-range translational order, and lipid lateral mobility is high. In the LC phase, the lateral diffusion coefficient is low and the orientational order of lipid chains is high. Lipid chains adopt hexagonal packing with substantial long-range translational ordering. The coexistence of LE and LC phases corresponds to a plateau region in the isotherm. The main advantage of simulating large systems is the ability to reproduce the phase coexistence region. The phase coexistence is not observed in the simulations of the small system. Small monolayers with the areas restricted in the phase coexistence interval correspond to a metastable state that has no equivalent in experimental systems. The coexistence of the LC and LE phases in the DPPC monolayer was also found in the atomistic simulations,[5] although the tension−area dependence was not reported.

The presence of a phase coexistence region of the isotherm is in good agreement with experiments; however, the monolayer tension in this region deviates slightly from the constant value, particularly near the phase boundaries. In experiments, the monolayer tension in the coexistence region may be not constant
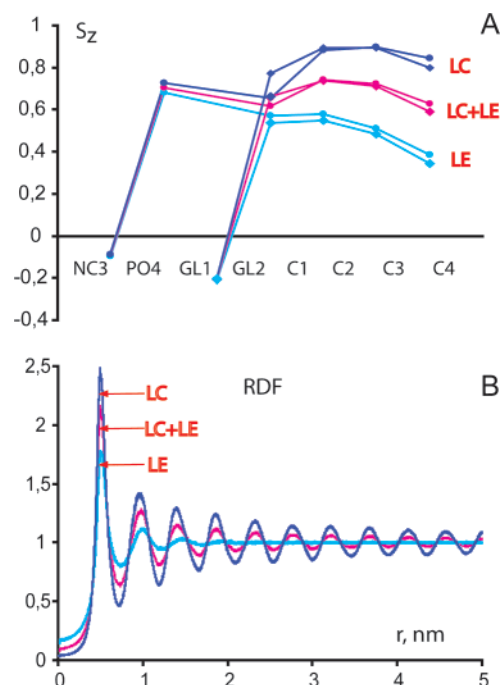
depending on the sizes and shapes of the domains, which are determined by the energy and entropy of mixing of the two phases.[25,26] Finite rates of monolayer compression may not allow the monolayer to equilibrate and thus affect the shape of the phase coexistence region. In the simulations, the system size ($\sim$50 $\times$ 50 nm^2) is too small to observe macroscopic phase coexistence. The domains cannot grow beyond the simulation box, and the equilibrium domain distribution cannot be obtained. In the calculated isotherm, the points at the plateau edges correspond to a metastable state, where the monolayer adopts only one phase (either LC or LE). According to two-dimensional nucleation theory,[27] the critical size of the nucleus of a new phase (characterizing the smallest cluster that will grow) and the time to create the nucleus increase near the phase coexistence boundaries. At the plateau edges, which correspond to the phase boundaries, either the critical size of a nucleus of LC (LE) phase is larger than the system size or the time to form the nucleus is longer than the simulation time.

In the coexistence region, the phase separation is complete and results in two domains of the LC and LE phases in each monolayer. The domains span the simulation box and form two infinite stripes. The monolayers with the coexisting LC and LE phases are anisotropic in the lateral direction. The line tension of the domain boundary between the LE and LC phases enters the calculated values of the monolayer tension because the force acting along the boundary contributes to the calculated pressure tensor. For example, if in both monolayers the two domains are oriented parallel to the x axis, then the line tension is related to the pressure tensor components, P_{xx} and P_{yy}, by the following approximate formula: $\lambda_m = 1/4 \cdot L_z L_y (P_{yy} - P_{xx})$, where the multiplier 1/4 accounts for two domain boundaries in the two monolayers in the simulation setup. The line tension between

(25) Israelachvili, J. *Langmuir* **1994**, *10*, 3774−3781.
(26) Ruckenstein, E.; Li, B. Q. *J. Phys. Chem. B* **1998**, *102*, 981−989.
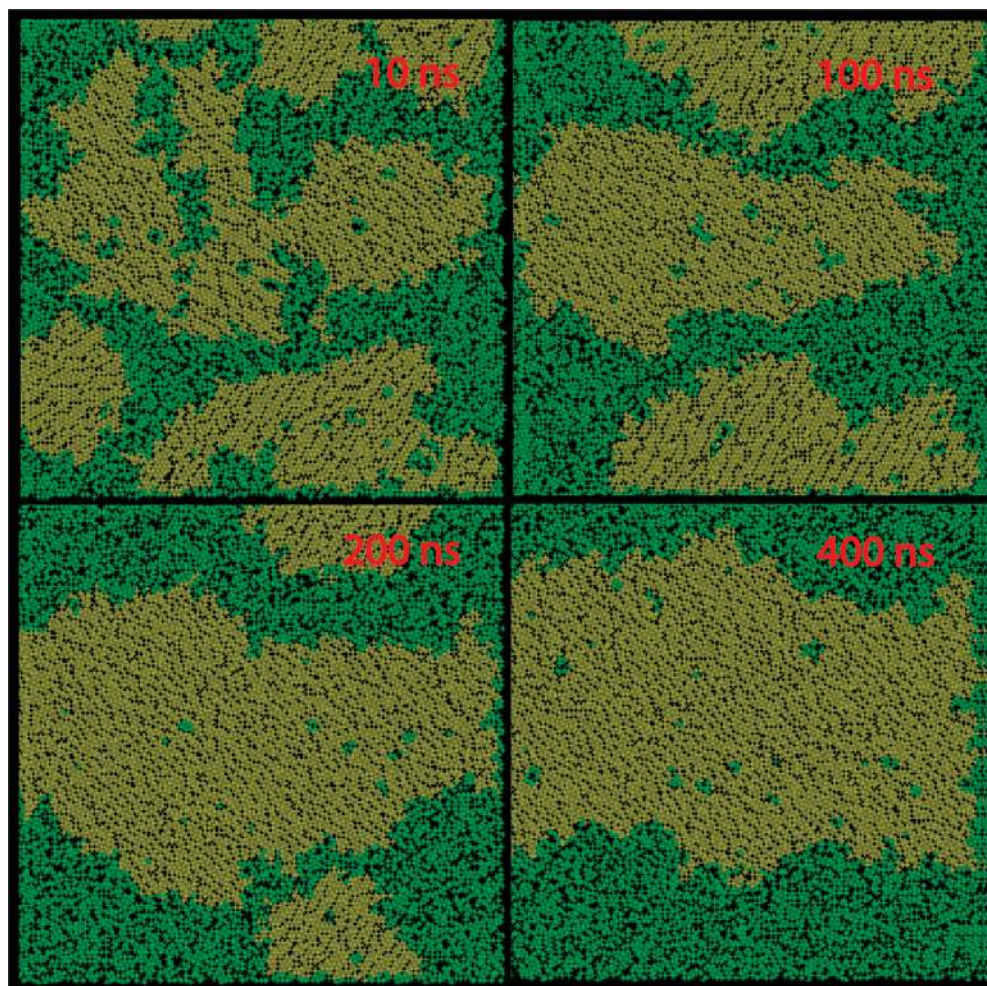(27) Atkins, P. W. *Physical Chemistry*, 5th ed.; Freeman: New York, 1994.

Figure 5. Coexistence of liquid-expanded (green) and liquid-condensed (yellow) phases in a DPPC monolayer at $A_L = 0.51$ nm². Distribution of lipids between domains is obtained using Voronoi analysis.
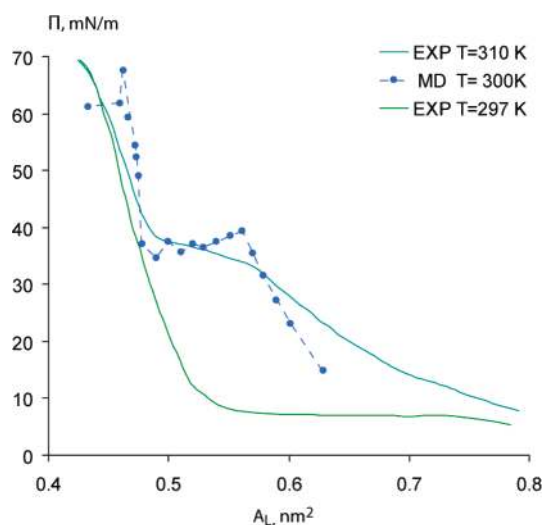

Figure 6. Pressure−area isotherms of a DPPC monolayer from molecular dynamics simulation (MD) and experiments (EXP, ref 14).

liquid-crystalline and gel domains in a DPPC bilayer in the CG model equals[13] $\lambda_b = 3$ pN. Assuming that the line tension of the domain boundaries in the monolayer is two times smaller than that of a bilayer, its contribution to the pressure is $P_{yy} - P_{xx} \approx 0.02$ bar. For comparison, the pressure tensor components at the coexistence plateau are $P_{xx} \approx P_{yy} \approx 5$ bar. Hence, the line tension between LC and LE phases is unlikely to give a substantial

contribution to the calculated values of the monolayer surface tension. In contrast, the anisotropic crystal-like properties of the LC phase do affect the monolayer surface tension. For a solid interface, the surface energy density is described by a surface stress tensor rather than a scalar surface tension because it depends on the orientation of the crystal. In the simulations, a LC domain in the monolayer adopts a specific orientation with respect to the simulation box axis. In the presence of a substantial proportion of LC phase in the monolayer, the nondiagonal component of the pressure tensor, P_{xy}, is not zero, $P_{xy} \approx 0.1$ bar, while the lateral pressure components are not equal, $P_{xx} - P_{yy} \approx \pm 1$ bar (error estimate for the pressure tensor components is <0.04 bar). Depending on the orientation of the LC domain, the pressure tensor components and thus the calculated value of the monolayer surface tension may differ. For the calculated isotherm, this difference is still small because the LC phase is not a solid crystal phase.

The slopes of the calculated isotherms on both sides of the plateau are somewhat steeper compared to experimental curves. A possible explanation for this is a finite size effect.[21] The slope of the tension−area curve is proportional to the area compressibility modulus of the monolayer, which is larger for smaller systems because of suppressed undulations and enhanced symmetry (due to the periodic boundary conditions).

At high compression, the monolayer surface first becomes rippled, then the monolayer bends and collapses. At the same time, the tension−area isotherm first decreases its slope and then

reaches the collapse plateau. This behavior is consistent with experimental observations.

In the expanded monolayers, there is a coexistence of the LE phase with pores. Pores are also observed in the experimental systems in the gas phase but at substantially larger areas per lipid. In the simulations, the monolayer surface tension decreases with increasing area per lipid in the LE−pores coexistence region. This is due to low surface tension at the vacuum−water interface, which stabilizes the pores and prevents the actual expansion of the monolayer. Low surface tension of the vacuum−water interface in the CG model is the result of the Lennard−Jones representation of the water particles. This representation does not fully model the entropy of water molecules, which is related to the orientation of the dipoles and hydrogen bonding. In the CG force field the underestimated entropic contribution is compensated by the enthalpic contribution to provide the correct free energies.

The partial entropic−enthalpic substitution used for the CG force field parametrization leads to weaker temperature depen-dence of the lipid properties. This can explain the underestimated temperature effect on the monolayer tension−area isotherm in the simulations.

However, these limitations of the model do not affect significantly the properties of the compressed monolayers (without pores) at a fixed temperature. Phase behavior of the lipid monolayers is well reproduced. The calculated tension−area isotherm can be compared to experimental pressure−area isotherms using a correction to the surface tension at the vacuum−water interface. Here, we used this correction in a simple form $\gamma_{aw}{}^* = \text{const}$, but it could also be chosen as a function of the area per lipid molecule, reflecting the degree of exposure of water molecules to vacuum in different points of the isotherm.

Conclusions

We calculated the entire pressure−area isotherm for a DPPC lipid monolayer using MD simulations with a realistic molecular model, which allows direct characterization of the monolayer structure, geometry, and phases and is in good agreement with experiments.